JACS
JOURNAL OF THE AMERICAN CHEMICAL SOCIETY

Subscriber access provided by UNIV NAC DE BUENOS AIRES

Article

How Mitogen-Activated Protein Kinases Recognize and Phosphorylate Their Targets: A QM/MM Study

Adrian Gustavo Turjanski, Gerhard Hummer, and J. Silvio Gutkind

J. Am. Chem. Soc., **Article ASAP** • DOI: 10.1021/ja8071995 • Publication Date (Web): 10 April 2009

Downloaded from http://pubs.acs.org on April 21, 2009

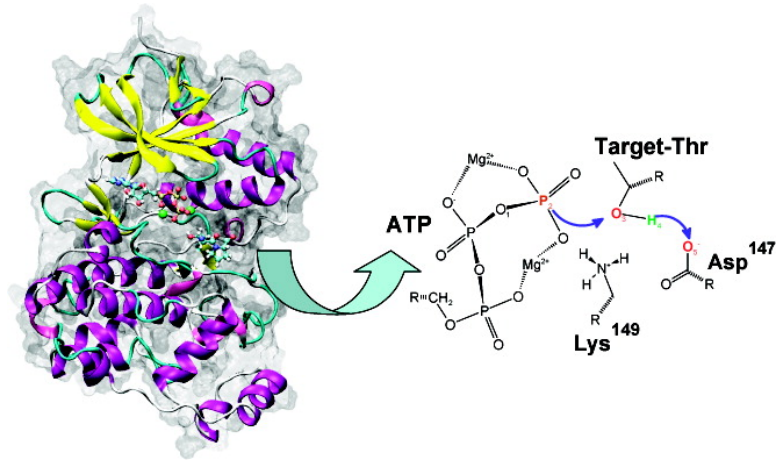

More About This Article

Additional resources and features associated with this article are available within the HTML version:

- Supporting Information
- Access to high resolution figures
- Links to articles and content related to this article
- Copyright permission to reproduce figures and/or text from this article

View the Full Text HTML

ACS Publications
High quality. High impact.

Journal of the American Chemical Society is published by the American Chemical Society. 1155 Sixteenth Street N.W., Washington, DC 20036

J|A|C|S
ARTICLES

How Mitogen-Activated Protein Kinases Recognize and Phosphorylate Their Targets: A QM/MM Study

Adrian Gustavo Turjanski,*,†,§ Gerhard Hummer,‡ and J. Silvio Gutkind†

Oral and Pharyngeal Cancer Branch, National Institute of Dental and Craniofacial Research, and Laboratory of Chemical Physics, National Institute of Diabetes and Digestive and Kidney Diseases, National Institutes of Health, Bethesda, Maryland 20892-0520

Received September 10, 2008; E-mail: adrian@qi.fcen.uba.ar

Abstract: Mitogen-activated protein kinase (MAPK) signaling pathways play an essential role in the transduction of environmental stimuli to the nucleus, thereby regulating a variety of cellular processes, including cell proliferation, differentiation, and programmed cell death. The components of the MAPK extracellular activated protein kinase (ERK) cascade represent attractive targets for cancer therapy, as their aberrant activation is a frequent event among highly prevalent human cancers. To understand how MAPKs recognize and phosphorylate their targets is key to unravel their function. However, these events are still poorly understood because of the lack of complex structures of MAPKs with their bound targets in the active site. Here we have modeled the interaction of ERK with a target peptide and analyzed the specificity toward Ser/Thr−Pro motifs. By using a quantum mechanics/molecular mechanics (QM/MM) approach, we propose a mechanism for the phosphoryl transfer catalyzed by ERK that offers new insights into MAPK function. Our results suggest that (1) the proline residue has a role in both specificity and phospho transfer efficiency, (2) the reaction occurs in one step, with ERK2 Asp^{147} acting as the catalytic base, (3) a conserved Lys in the kinase superfamily that is usually mutated to check kinase activity strongly stabilizes the transition state, and (4) the reaction mechanism is similar with either one or two Mg^{2+} ions in the active site. Taken together, our results provide a detailed description of the molecular events involved in the phosphorylation reaction catalyzed by MAPK and contribute to the general understanding of kinase activity.

Introduction

Mitogen-activated protein kinase (MAPK) signaling cascades[1] play an essential role in the transduction of environmental stimuli to the nucleus, regulating the expression of genes involved in a variety of cellular processes, including cell proliferation, differentiation, programmed cell death, and neoplastic transformation.[2−4] MAPKs have been classified into at least six subfamilies, among which the extracellular activated protein kinases ERK/MAPKs (ERK1 and ERK2) are the most extensively studied. The aberrant activation of the ERK pathway has been shown to be a frequent event in many human tumor types.[5,6] As this pathway is an attractive target for cancer chemotherapy, interest in the components of the ERK signaling pathway has exploded in the past few years (see the review in ref 7 and references therein).

MAPKs are characterized by their requirement of a dual phosphorylation at conserved threonine (Thr) and tyrosine (Tyr) residues for activation[8−10] and their specific activity toward serine (Ser)/Thr residues followed by proline (Pro).[11] Structural and biochemical studies have extensively characterized the activation process and the catalytic activity of MAPKs, providing compelling evidence that MAPKs facilitate substrate recognition through docking interactions outside the active site.[12] However, the origin of Pro selectivity and the phospho transfer mechanism are not clearly understood, mainly because of a lack of structures of these kinases with targets bound in the active site. In this work, we have used computational tools to model the complex of ERK2 with a target peptide and analyzed the phosphoryl transfer reaction mechanism in detail. On the basis of the wealth of structural information on MAPKs and other

† National Institute of Dental and Craniofacial Research.
‡ National Institute of Diabetes and Digestive and Kidney Diseases.
§ Current address: Departamento de Química Inorgánica, Analítica y Química Física e INQUIMAE y Departamento de Química Biológica, Facultad de Ciencias Exactas y Naturales, UBA, Buenos Aires, Argentina.

(1) Raman, M.; Chen, W.; Cobb, M. H. *Oncogene* **2007**, *26*, 3100–3112.
(2) Chang, L.; Karin, M. *Nature* **2001**, *410*, 37–40.
(3) Weston, C. R.; Davis, R. J. *Curr. Opin. Cell. Biol.* **2007**, *19*, 142–149.
(4) Kyriakis, J. M.; Avruch, J. *Physiol. Rev.* **2001**, *81*, 807–869.
(5) Gioeli, D.; Mandell, J. W.; Petroni, G. R.; Frierson, H. F., Jr.; Weber, M. J. *Cancer Res.* **1999**, *59*, 279–284.
(6) Hoshino, R.; Chatani, Y.; Yamori, T.; Tsuruo, T.; Oka, H.; Yoshida, O.; Shimada, Y.; Ari-i, S.; Wada, H.; Fujimoto, J.; Kohno, M. *Oncogene* **1999**, *18*, 813–822.
(7) Lawrence, M. C.; Jivan, A.; Shao, C.; Duan, L.; Goad, D.; Zaganjor, E.; Osborne, J.; McGlynn, K.; Stippec, S.; Earnest, S.; Chen, W.; Cobb, M. H. *Cell Res.* **2008**, *18*, 436–442.
(8) Payne, D. M.; Rossomando, A. J.; Martino, P.; Erickson, A. K.; Her, J. H.; Shabanowitz, J.; Hunt, D. F.; Weber, M. J.; Sturgill, T. W. *EMBO J.* **1991**, *10*, 885–92.
(9) Robinson, M. J.; Cheng, M.; Khokhlatchev, A.; Ebert, D.; Ahn, N.; Guan, K. L.; Stein, B.; Goldsmith, E.; Cobb, M. H. *J. Biol. Chem.* **1996**, *271*, 29734–29739.
(10) Canagarajah, B. J.; Khokhlatchev, A.; Cobb, M. H.; Goldsmith, E. J. *Cell* **1997**, *90*, 859–869.
(11) Clark-Lewis, I.; Sanghera, J. S.; Pelech, S. L. *J. Biol. Chem.* **1991**, *266*, 15180–15184.
(12) Remenyi, A.; Good, M. C.; Lim, W. A. *Curr. Opin. Struct. Biol.* **2006**, *16*, 676–685.

 © XXXX American Chemical Society

kinases, we assembled the catalytic site of ERK2, which enabled us to study the phospho transfer process using hybrid quantum mechanics/molecular mechanics (QM/MM) computational schemes.[13−15]

Our results indicate that specificity for Pro in the phospho acceptor site may be due to binding restrictions and the fixed positioning of the target residue, suggesting a role in the MAPK catalytic activity in addition to its importance for substrate recognition. The reaction mechanism of members of the kinase superfamily has been extensively studied.[16,17] Nevertheless, the detailed chemical mechanism of catalysis remains a matter of controversy. Analysis of the MAPK reaction mechanism using QM/MM tools shows that (1) the ERK2-catalyzed reaction occurs in one step, (2) a conserved aspartic acid (Asp^{147} in ERK2) acts as the catalytic base, and (3) a lysine (Lys^{149} in ERK2) residue conserved in the kinase superfamily forms strong interactions with the γ-phosphate along the reaction pathway, thereby providing the right positioning of the ATP and stabilizing the transition state. Our computational model also enabled us to investigate the contribution of different residues within the MAPK active site to the catalytic efficiency. Overall, our emerging results are aligned with previous experimental studies of MAPKs.[17−21] Together, the results presented here provide a detailed description of the phosphorylation reaction catalyzed by ERK2 that enhances our ability to understand MAPK function and inhibition.

Materials and Methods

Complex Preparation. There is currently no experimental structure of active WT ERK with ATP and Mg^{2+} cations in a conformation suitable for catalysis. For our study, we started by reconstructing the ERK−ATP−Mg^{2+} complex, after which we docked the target peptide and relaxed the whole complex. We used the crystal structures of the protein ERK2 [Protein Data Bank (PDB)[22] code 2ERK[10]] as the starting point for our calculations. The structures of other MAPK−ATP−Mg^{2+} complexes (P38-γ[23] and JNK3[24]) and biochemical experiments suggest that ERK2 can bind two Mg^{2+} ions.[20] Accordingly, we generated a complex of activated ERK2 with ATP and two Mg^{2+} cations in the active site. For the positioning of ATP and the two Mg^{2+} ions, we used the ERK2−ATP complex (PDB code 1GOL[21]) and the P38-γ ATP complex (PDB code 1CM8[23]). The 1GOL structure has a distorted ATP because of the K52R mutation and the presence of only one Mg^{2+} ion, whereas 1CM8 has two Mg^{2+} ions and the ATP in a conformation suitable for catalysis. All of the classical simulations were performed with the AMBER-99 force field[25] and the AMBER 8 package.[26] The system was solvated with an isometric truncated octahedron of TIP3P[27] water molecules and neutralized by the addition of K^+ cations. The parameters for phosphotyrosine and phosphoserine were taken from Craft and Legge[28] and the ATP parameters from Meagher et al.[29] The time step was 2 fs. The particle-mesh Ewald method[30] was used with a nonbonded cutoff of 12 Å, and the Berendsen thermostat[31] was used to maintain the desired temperature. All of the hydrogen bonds were kept rigid by using the SHAKE algorithm.[32]

The structure of ERK2−ATP was first equilibrated at 300 K for 100 ps while keeping the whole protein fixed to allow the water and ligand molecules to relax. As a restraint we used a harmonic potential with a force constant of 4 kcal mol^{-1} $Å^{-2}$. In a subsequent 500 ps molecular dynamics (MD) simulation without restraints, the entire system was allowed to relax and equilibrate. The final snapshot was used as the starting point for modeling the peptide−protein interaction.

The complex of ERK2−ATP with the model tripeptide CH_3CO−Ala−Thr−Pro−$NHCH_3$ as the substrate was assembled by first substituting the OH group of Thr in place of a water molecule that during the dynamics remained located near the γ-phosphate of ATP; this is a position similar to the one found for Ser in other kinase−ligand complexes.[33] It should be noted that peptides longer than the tripeptide modeled in this study are used in experimental measurements of the enzymatic activity of MAPKs. This is because peptides lacking the docking motifs have only a low affinity toward MAPKs. However, these docking motifs affect binding affinity but not catalytic activity, as they bind to docking-motif binding sites that are far from the catalytic site. Thus, to understand the MAPK reaction mechanism, short peptides bound into the catalytic site should prove sufficient. Among several different trial conformers for the Pro residue following Thr, only *trans*-Pro left the OH of Thr in the right position and did not produce clashes with other residues of ERK2. We conducted a 200 ps MD simulation at 300 K, keeping the whole protein and peptide fixed, followed by a 500 ps simulation allowing the whole system to relax, which helped accommodate the ATP, the peptide, and the C-terminal and N-terminal domains for efficient catalysis. We minimized the energy of the resulting structure by simulated annealing and conjugate gradient search. The QM/MM calculations were initiated from the resulting complex structure, including water molecules within a sphere of 45 Å from the center of the Mg cations.

To explore the role of the two Mg^{2+} cations in the reaction process, we performed additional calculations in which one of the ions was moved from the active site to the water solvent. To characterize the specific effect of the Mg^{2+} ion and maintain electroneutrality, the ion was exchanged with a classical water molecule located near the active site but remained part of the QM subsystem. We relaxed the system by conducting short 200 ps MD simulations with restraints acting on residues more than 8 Å away from the active site.

QM/MM Methods. The QM computations were performed with the SIESTA code[34] at the density functional theory (DFT) level.

(13) Friesner, R. A.; Guallar, V. *Annu. Rev. Phys. Chem.* **2005**, *56*, 389–427.
(14) Mulholland, A. J.; Grant, G. H.; Richards, W. G. *Protein Eng.* **1993**, *6*, 133–147.
(15) Sanchez, V. M.; Crespo, A.; Gutkind, J. S.; Turjanski, A. G. *J. Phys. Chem. B* **2006**, *110*, 18052–18057.
(16) Cheng, Y.; Zhang, Y.; McCammon, J. A. *J. Am. Chem. Soc.* **2005**, *127*, 1553–1562.
(17) Wang, Z. X.; Wu, J. W. *J. Biol. Chem.* **2007**, *282*, 27678–27684.
(18) Prowse, C. N.; Hagopian, J. C.; Cobb, M. H.; Ahn, N. G.; Lew, J. *Biochemistry* **2000**, *39*, 6258–6266.
(19) Waas, W. F.; Rainey, M. A.; Szafranska, A. E.; Dalby, K. N. *Biochemistry* **2003**, *42*, 12273–12286.
(20) Waas, W. F.; Dalby, K. N. *Biochemistry* **2003**, *42*, 2960–2970.
(21) Robinson, M. J.; Harkins, P. C.; Zhang, J.; Baer, R.; Haycock, J. W.; Cobb, M. H.; Goldsmith, E. J. *Biochemistry* **1996**, *35*, 5641–5646.
(22) Berman, H. M.; et al. *Acta Crystallogr., Sect. D.: Biol. Crystallogr.* **2002**, *58*, 899–907.
(23) Bellon, S.; Fitzgibbon, M. J.; Fox, T.; Hsiao, H. M.; Wilson, K. P. *Structure* **1999**, *7*, 1057–1065.
(24) Xie, X.; Gu, Y.; Fox, T.; Coll, J. T.; Fleming, M. A.; Markland, W.; Caron, P. R.; Wilson, K. P.; Su, M. S. *Structure* **1998**, *6*, 983–991.
(25) Wang, J. M.; Cieplak, P.; Kollman, P. A. *J. Comput. Chem.* **2000**, *21*, 1049–1074.
(26) Case, A.; et al. *Amber 7*; University of California: San Francisco, 2002.
(27) Jorgensen, W. L.; Chandrasekhar, J.; Madura, J. D.; Impey, R. W.; Klein, M. L. *J. Chem. Phys.* **1983**, *79*, 926–935.
(28) Craft, J. W., Jr.; Legge, G. B. *J. Biomol. NMR* **2005**, *33*, 15–24.
(29) Meagher, K. L.; Redman, L. T.; Carlson, H. A. *J. Comput. Chem.* **2003**, *24*, 1016–1025.
(30) Essmann, U.; Perera, L.; Berkowitz, M. L.; Darden, T.; Lee, H.; Pedersen, L. G. *J. Chem. Phys.* **1995**, *103*, 8577–8593.
(31) Berendsen, H. J. C.; Postma, J. P. M.; Vangunsteren, W. F.; Dinola, A.; Haak, J. R. *J. Chem. Phys.* **1984**, *81*, 3684–3690.
(32) Ryckaert, J. P.; Ciccotti, G.; Berendsen, H. J. C. *J. Comput. Phys.* **1977**, *23*, 327–341.
(33) Brown, N. R.; Noble, M. E.; Endicott, J. A.; Johnson, L. N. *Nat. Cell Biol.* **1999**, *1*, 438–443.

For all of the atoms in the QM subsystem, basis sets of double-ζ plus polarization quality were employed, with a pseudoatomic orbital energy shift of 25 meV and a grid cutoff of 150 Ry. The basis functions consisted of localized (numerical) pseudoatomic orbitals that were projected on a real-space grid to compute the Hartree potential and exchange correlation potential matrix elements. Calculations were performed using the generalized gradient approximation functional proposed by Perdew, Burke, and Ernzerhof.[35] The classical subsystem was treated using the parametrization from the AMBER force field.[25] The interface between the QM and MM portions of the system was treated by the scaled position link atom method[36,37] adapted to the SIESTA code.[38]

We used two different QM subsystems in our study. The "small" QM subsystem consisted of the triphosphate part of ATP, the two Mg^{2+} cations, the side chain of Asp^{147}, the $CH_2NH_3^+$ part of the side chain of Lys^{149}, and the side chain of the Thr of the target peptide, for a total of 43 atoms. For the "large" subsystem, we considered the small subsystem plus all of the target tripeptide atoms, giving a total of 84 atoms. To explore possible differences between Ser and Thr phosphorylation, we mutated the Thr in the peptide to a Ser and used the small QM subsystem to evaluate the differences. The rest of the ERK2 protein, together with water molecules, was treated classically. To separate the QM and MM subsystems, atoms in the side chains of Asp^{147} and Lys^{149}, the ATP triphosphate moiety, and the side chain of the target Thr or Ser were used as link atoms.

The complexes obtained from the MD simulations were further relaxed by hybrid QM/MM geometry optimizations using a conjugate gradient algorithm. Only residues located within 8 Å of any QM atom were allowed to move freely in the QM/MM runs. We then computed the potential energy profiles using restrained energy minimizations along the selected reaction paths. For this purpose, an additional term was added to the potential energy: $V(\varepsilon) = k(\varepsilon - \varepsilon_0)^2/2$, where k is an adjustable force constant, ε is the value of the reaction coordinate in the particular system configuration, and ε_0 is the target value of the reaction coordinate. Varying ε_0 forced the system to follow a low-energy reaction path along the given coordinate.

Results

Target Binding Specificity. MAPKs are composed of two domains,[39] an N-terminal domain formed largely by β-sheets and a C-terminal domain that is mostly helical, with four short β-strands [see Figure 1A depicting the complex of active ERK2 (PDB code 2ERK[10]) with ATP and two Mg^{2+} cations and a tripeptide $CH_3CO-Ala-Thr-Pro-NHCH_3$ as the substrate]. The catalytic site, where the ATP and one or two Mg ions bind, is at the junction between these two domains (Figure 1A).[39] Upon phosphorylation, a conformational change in the activation lip of ERK2 opens up the catalytic site and exposes a hydrophobic pocket to the solvent.[10] In our model, the small peptide is bound in this hydrophobic pocket, making specific interactions with ERK2.

Our model of the complex provides insights into the molecular basis of the sequence specificity for the peptide target. We found that the consensus Pro is in a trans conformation that helps position the target Thr deep into the catalytic site. Pro interacts with the aromatic side chain of the phosphorylated tyrosine (Tyr^{185}) (Figure 1B) and the side chain of leucine (Leu^{168}). With backbone dihedral angles $\omega = -170°$, $\varphi = -78°$, and $\psi = 30°$, Pro has an α-helical conformation, as previously observed in an isolated TSPI peptide.[40] To explore the molecular basis of the specificity of MAPKs toward Pro, we tested the possibility of having different amino acids at the Pro position C-terminal to the phosphorylation site. When the target Thr was kept near the ATP, introduction of bulkier amino acids at the Pro site resulted in clashes with the phosphorylated Tyr, which is tightly bound to the arginines Arg^{189} and Arg^{192}. Even Val, which is structurally similar to Pro, did not fit. When we mutated Pro to Val in the docked peptide, one of the methyl groups of Val clashed with the side chain of the phospho-Tyr. In contrast, the smaller amino acids glycine (Gly) or alanine (Ala) lack the rigidity to keep the Thr deeply bound into the binding pocket, resulting in significant Thr movement away from the ATP upon unrestrained minimization of the mutated peptides. Indeed, in our QM/MM simulations (see below), we found that the distance between the target oxygen and the ATP is critical for the barrier height. These differences affect the positioning of the peptide in the active site, which helps explain previous experiments in which mutations of Pro to Ala and Gly in the ERK substrate EtsΔ138 produced 5- and 20-fold reductions, respectively, in the catalysis rate constant k_{cat}.[41]

Comparison of our model with CDK2−peptide complexes shows similar features overall. However, one important difference is the presence of the phospho-Tyr^{185} in ERK2 that makes a smaller binding site for Pro. This difference could be reflected in the fact that CDK2 also recognizes a positive residue (Lys

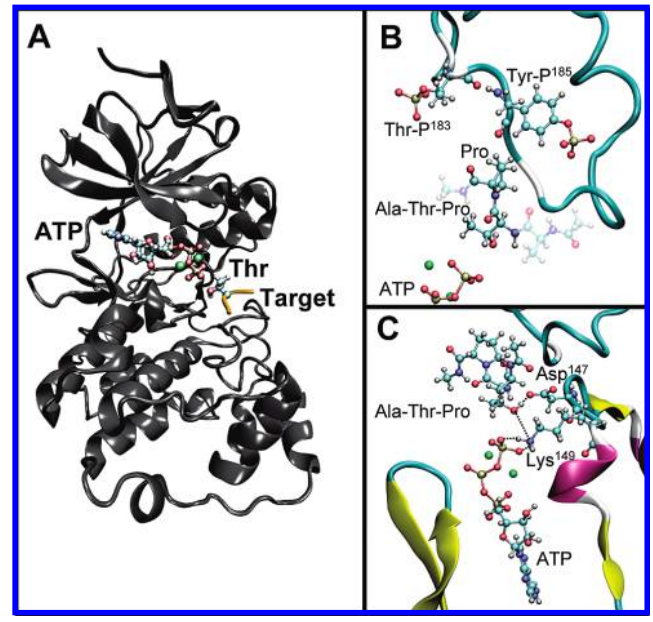

Figure 1. (A) Structure of active ERK2 (gray ribbon rendering) complexed with ATP and two Mg^{2+} cations (ball-and-stick rendering) and the target peptide (yellow), with the Thr shown in the ball-and-stick representation. (B) Details of the complex structure, showing the Pro conformation and the phospho-Ser and phospho-Tyr residues (ball-and-stick rendering). (C) Another view of the complex, showing the interactions of the target Thr with the conserved Asp^{147} and Lys^{149}.

(34) Soler, J. M.; Artacho, E.; Gale, J. D.; Garcia, A.; Junquera, J.; Ordejon, P.; Sanchez-Portal, D. *J. Phys.: Condens. Matter* **2002**, *14*, 2745–2779.
(35) Perdew, J. P.; Burke, K.; Ernzerhof, M. *Phys. Rev. Lett.* **1996**, *77*, 3865–3868.
(36) Eichinger, M.; Tavan, P.; Hutter, J.; Parrinello, M. *J. Chem. Phys.* **1999**, *110*, 10452–10467.
(37) Rovira, C.; Schulze, B.; Eichinger, M.; Evanseck, J. D.; Parrinello, M. *Biophys. J.* **2001**, *81*, 435–445.
(38) Crespo, A.; Scherlis, D. A.; Marti, M. A.; Ordejon, P.; Roitberg, A. E.; Estrin, D. A. *J. Phys. Chem. B* **2003**, *107*, 13728–13736.
(39) Chen, Z.; Gibson, T. B.; Robinson, F.; Silvestro, L.; Pearson, G.; Xu, B.; Wright, A.; Vanderbilt, C.; Cobb, M. H. *Chem. Rev.* **2001**, *101*, 2449–2476.
(40) Hamelberg, D.; Shen, T.; McCammon, J. A. *J. Am. Chem. Soc.* **2005**, *127*, 1969–1974.

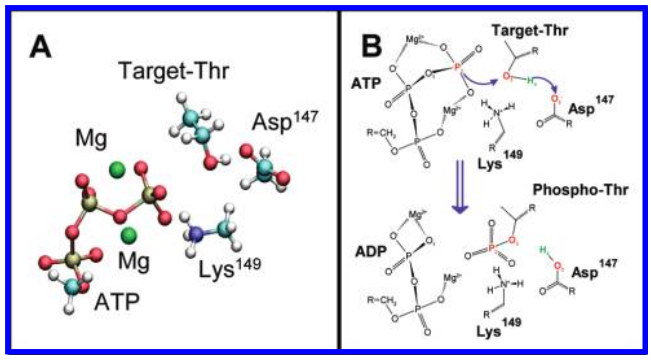

Figure 2. (A) Small QM subsystem used in the QM/MM calculations. (B) Scheme depicting the movements of the atoms in the phosphoryl transfer process.

or Arg) apart from Pro,[33] a feature that MAPKs lack. Another important characteristic of Pro is the lack of the backbone NH group; interestingly, there is no polar group of ERK2 that enables the formation of a hydrogen bond in that position, which suggests that the binding of amino acids other than Pro would be energetically unfavorable, as has been shown in CDK2 and suggested for ERK2.[10,33] Ala^{187} in ERK2 has a left-handed conformation similar to that of Val^{164} in CDK2, which results in the carbonyl oxygen atom being directed away from the substrate. In summary, our results for the complex structure suggest that Pro has two roles in ensuring MAPK specificity: binding deep into the pocket in a rigid structure for efficient catalysis and recognition by specific interactions.

The target peptide and ATP interact with several key residues of ERK2. The OH group of Thr forms a tight hydrogen bond with Asp^{147}, with an O−O distance of 2.6 Å. Lys^{149} is strongly bound to the γ-phosphate of ATP via two salt bridges and also interacts with the target Thr, as the basic nitrogen is only 3.1 Å apart from the hydroxyl oxygen (Figure 1C). Two possible binding sites for Mg^{2+} ions in Ser/Thr kinases have been proposed: M1, where the cation is coordinated by two oxygen atoms from the β- and γ-phosphates of ATP, the acidic oxygen atoms of a conserved Asp, and two water molecules; and M2, where the Mg^{2+} cation is coordinated by two oxygen atoms from the α- and γ-phosphates of ATP, one oxygen from the conserved Asp, one oxygen from a conserved Asn, and a water molecule.[42] In our model of ERK2, Mg^{2+} binding is similar to that observed in P38:[23] Asp^{165} coordinates both Mg^{2+} cations, and Asn^{152} interacts with the M2 Mg^{2+} site.

Phosphorylation Mechanism. We performed QM/MM calculations to explore the mechanism of the phospho transfer reaction from ATP to the Thr of the bound peptide catalyzed by the phosphorylated (active) ERK2. We considered the QM subsystem depicted in Figure 2A; the system includes the triphosphate part of ATP, the two Mg^{2+} atoms, and the side chains of Asp^{147}, Lys^{149}, and Thr of the target peptide, resulting in a total of 43 atoms.

We considered two possible reaction mechanisms, with either the ATP γ-phosphate or Asp^{147} acting as the proton acceptor from the target Thr. As the reaction involves the rupture of the ATP γ-phosphate bond and the Thr OH bond as well as the formation of the phosphate Thr bond and the hydrogen (H_4) Asp^{147} or γ-phosphate bond, a natural reaction coordinate should be the simple coordinate $d(O_1-P_2) - d(P_2-O_3)$. However, we found that with this coordinate, H_4 was not transferred and the energy went continuously up, resulting in an unproductive reaction (data not shown). We then tried the more complex reaction coordinate $d(O_1-P_2) + d(O_3-H_4) - d(P_2-O_3) - d(H_4-O_5)$ (Figure 2B), where Asp^{147} acts as the proton acceptor. With this coordinate, we obtained a complete reaction profile with a reasonable activation barrier. However, when we examined the transfer of the Thr OH hydrogen atom to an oxygen atom of the γ-phosphate group of ATP instead of Asp^{147}, we failed to obtain stable products (not shown), which is probably caused by a high energy barrier.

For the reaction with Asp^{147} as the acceptor, the conformations of the reactant, transition, and product states are depicted in Figure 3A−C. The energy as a function of the reaction coordinate is shown in Figure 4A, with an activation barrier of 17.1 kcal/mol. The changes in the most relevant distances as a function of the reaction coordinate are shown in Figure 4B and summarized in Table 1. The reaction pathway involves the breaking of the O_1-P_2 bond and the concomitant formation of the P_2-O_3 bond. The O_1-P_2 bond lengthens from 1.80 to 2.43 Å in going from the reactant state to the transition state, while the P_2-O_3 distance is reduced from 3.60 to 2.43 Å (Figure 4B). At the beginning of the reaction path, the Thr moves toward the ATP, accompanied by only a modest increase in the O_1-P_2 distance; only as the Thr OH moiety is brought within ~3 Å of the γ-phosphate does the O_1-P_2 bond start to break. At the transition state, the γ-phosphate PO_3 becomes planar and symmetrical, with identical P_2-O_1 and P_2-O_3 distances of ~2.4 Å (Table 1). By using the analysis suggested by Mildvan,[43] we found that the reaction has ~90% dissociative character, which is in agreement with the results of similar studies on PKA.[16,44]

A key step in the reaction is the proton transfer from Thr to Asp^{147}. Interestingly, we find that the H^+ is only transferred when the P_2-O_3 bond is almost fully formed (Figure 4B). For ERK2, our results thus argue against an alternative scenario in which a low-barrier hydrogen transfer to the nearby Asp occurs at an early stage of the phospho transfer process.[45] During the reaction, Lys^{149} rotates and remains in contact with the γ-phosphate as it is transferred to Thr.

The calculations using the small QM system clearly point toward a specific phosphorylation mechanism. However, the energy difference of 14.3 kcal/mol between the reactant and product states is unrealistic (Figure 4A). A likely cause is that the phosphate is being transferred to a relatively small QM-treated moiety, CH_3CH_2OH. To explore this effect and possible changes in the mechanism, we performed additional calculations with the large QM system, which encompassed the small QM subsystem plus the entire target tripeptide (84 atoms total) (Figure 5A). We used the same reaction coordinate as for the small QM subsystem and found no significant differences in the reaction mechanism. However, we obtained a significantly lower activation barrier of 13.8 kcal/mol (Figure 5B and Table 1), representing a stabilization of 3.3 kcal/mol with respect to the result using the small QM subsystem. The main factor in this difference appears to be the stabilization of the phosphorylated product state. The shape of the potential energy curve

(41) Rainey, M. A.; Callaway, K.; Barnes, R.; Wilson, B.; Dalby, K. N. *J. Am. Chem. Soc.* **2005**, *127*, 10494–10495.
(42) Zheng, J.; Knighton, D. R.; ten Eyck, L. F.; Karlsson, R.; Xuong, N.; Taylor, S. S.; Sowadski, J. M. *Biochemistry* **1993**, *32*, 2154–2161.
(43) Mildvan, A. S. *Proteins* **1997**, *29*, 401–416.
(44) Valiev, M.; Yang, J.; Adams, J. A.; Taylor, S. S.; Weare, J. H. *J. Phys. Chem. B* **2007**, *111*, 13455–13464.
(45) De Vivo, M.; Cavalli, A.; Carloni, P.; Recanatini, M. *Chemistry* **2007**, *13*, 8437–8444.

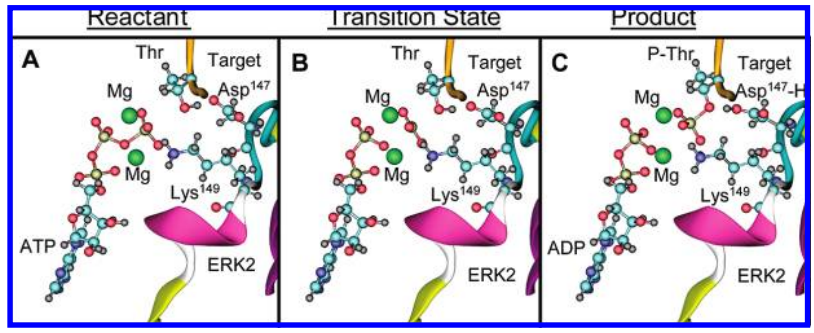

Figure 3. Structures of the (A) reactants, (B) transition state, and (C) products determined for the ERK2-catalyzed reaction. ATP, the Mg^{2+} cations, and the conserved Asp^{147} and Lys^{149} are depicted in ball-and-stick rendering.

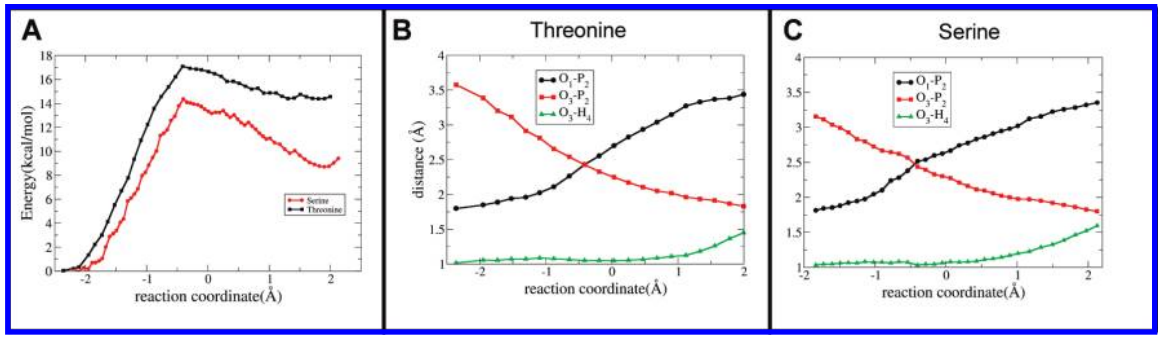

Figure 4. (A) Change in potential energy as a function of the reaction coordinate for (black) Thr or (red) Ser phosphorylation, as determined by the QM/MM calculations using the small QM subsystem. (B, C) Changes in relevant bond distances as a function of the reaction coordinate for (B) Thr and (C) Ser phosphorylation.

Table 1. Calculated Activation Energies E_a (kcal/mol), Changes in Mulliken Charges Δq (e), and Selected Optimized Distances d (Å) for the Selected Model Systems[a]

	small Thr			small Ser			small $1Mg^{2+}$			large WT			large K52A		
E_a	17.1			14.1			5.0			13.8			19.5		
	R	TS	P	R	TS	P	R	TS	P	R	TS	P	R	TS	P
$d(O_1-P_2)$	1.80	2.43	3.41	1.81	2.48	3.31	1.87	2.56	3.43	1.77	2.39	3.30	1.79	2.41	3.32
$d(P_2-O_3)$	3.60	2.43	1.83	3.15	2.46	1.81	3.50	2.61	1.84	3.54	2.39	1.79	3.66	2.41	1.80
$d(O_3-H_4)$	1.01	1.05	1.46	1.03	1.04	1.58	1.00	1.02	1.49	1.02	1.06	1.60	1.02	1.15	1.59
$\Delta q(ADP)^b$	0.00	−0.38	−0.46	0.00	−0.41	−0.51	0.00	−0.27	−0.47	0.00	−0.49	−0.55	–	–	–
$\Delta q(Asp^{147})^b$	0.00	0.01	0.36[c]	0.00	0.04	0.54[c]	0.00	0.05	0.61	0.00	0.20	0.65[c]	–	–	–

[a] Abbreviations: R, reactants; TS, transition state; P, products. [b] Change in the net Mulliken charge of the selected moiety relative to that of the reactants. [c] The product includes the charge of the transferred H_4.

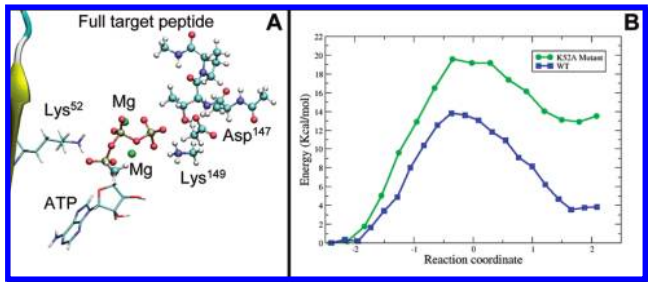

Figure 5. (A) Large QM subsystem used in the QM/MM calculations (ball-and-stick rendering) showing the ATP moiety and the position of Lys^{52} (stick rendering). (B) Change in potential energy as a function of the reaction coordinate for the wild-type enzyme (WT) and the Lys^{52} mutant (K52A) using the large QM subsystem.

shows a remarkable stabilization of the phosphorylated peptide relative to the result for the small QM subsystem. The difference in the potential energies of the reactants and products is 3.2 kcal/mol, showing that using the large QM subsystem including all of the peptide atoms stabilized the formation of the phospho-Thr product.

To further explore the role of the different groups in the reaction, we performed a qualitative analysis of the Mulliken charge distributions for the reactant, transition, and product states for the two models that we used. We also analyzed the potential factors lowering the barrier for the phospho transfer and stabilizing the ERK2-bound product state in the larger subsystem. Presumably, the γ-phosphate oxygen atoms could increase the nucleophilicity of the substrate hydroxyl group to attack P_3. In agreement with this idea, our results show that upon formation of the complex, the Thr target receives an extra charge of $-0.2e$ from the enzyme. At the transition state, the leaving phosphate retains part of its negative charge; however, there is a significant decrease of $\sim 0.2e$, with a marked change of $0.1e$ in the P_3 charge that is opposed to the extra charge of $-0.4e$ and $-0.5e$ gained by the ADP moiety using the small and large QM subsystems, respectively (Table 1). The charge of Lys^{149} does not significantly change in the reaction, which suggests that its main role is to position the ATP for catalysis

Scheme 1

$$E + S + ATP \underset{k_{-2}}{\overset{k_2}{\rightleftharpoons}} E{-}S{-}ATP \xrightarrow{k_3}$$

$$E{-}P{-}ADP \xrightarrow{k_4} E + P + ADP$$

and possibly to stabilize the leaving γ-phosphate along the reaction path. The most striking observed difference between the two models is the charge of Asp^{147}; a significant increase ($0.2e$) in its charge upon formation of the transition state is obtained only for the large QM subsystem, suggesting that even though the hydrogen transfer has not begun at this point, there is a charge transfer from the Thr to Asp^{147} at an early stage of the reaction. This implies that the conserved Asp in the kinase superfamily may have a role in determining the activation barrier by accepting charge from the target.

Detailed kinetic analyses of the phosphoryl transfer reaction catalyzed by ERK2 allowed us to relate our results to available experimental information.[17−19] The suggested ERK2 reaction pathway is shown in Scheme 1; on the basis of solvent viscometric techniques, it has been proposed that the rate-limiting step of the reaction is the phospho transfer step (with rate constant k_3).[18] However, a recent study proposed that both the phosphoryl transfer (k_3) and substrate release (k_4) steps are rate-limiting.[17] Reported values for k_3 are between 10 and 40 s^{-1}.[17,18] A transition state theory estimate of ~15.0 kcal/mol for the reaction barrier was obtained, which is in reasonable agreement with our results assuming a prefactor of ~1 ps^{-1}.

In summary, we propose a reaction mechanism for ERK2 that involves the dissociation of the γ-phosphate from ATP with the concomitant formation of the phosphopeptide. The proton transfer to the conserved Asp occurs late in the reaction process, but partial charge transfer to Asp occurs upon formation of the transition state. Our study provides a detailed description of the phosphorylation catalyzed by MAPKs and therefore broadens our understanding of their function. Is important to remark that the mechanism proposed here is in agreement with previous experimental results.[17,18]

Ser versus Thr Phosphorylation. We performed a comparative study by replacing the Thr residue in the target peptide by Ser using the small QM subsystem as a reference. A significant difference in the activation energy was found for Ser phosphorylation: the value of 14.1 kcal/mol represents a decrease of 3.0 kcal/mol relative to that for Thr (Figure 4A). However, the reaction mechanism for Ser, as judged by the changes in the most relevant reaction coordinates (Figure 4C), is very similar to that for Thr. The most striking difference is that the OH group of the smaller Ser is closer to the ATP than that of the Thr peptide, as indicated by a reactant $O_3{-}P_2$ distance of ~3.15 Å as opposed to ~3.60 Å for Thr (Figure 4C). These results point out the importance of the ability of Pro to direct the target for efficient catalytic activity. Another important difference is the remarkable stabilization of phospho-Ser with respect to phospho-Thr (~6.4 kcal/mol). Analysis of the changes in the Mulliken charges along the reaction path may explain some of the observed differences. Most of the charge changes are similar to those observed before for Thr. However, the charge of the protonated Asp^{147} in the product state is less negative by ~$0.2e$ than in the Thr case, which may explain the gain in relative stability of the products. The combination of both a decrease in the $O_3{-}P_2$ reactant distance and a stabilization of the product state may explain the reduced activation energy observed for Ser.

MAPKs can phosphorylate either Ser or Thr residues in their different targets.[39] However, it is not known whether there are differences in the reaction steps (k_2, k_{-2}, k_3, and k_4 in Scheme 1) for Ser as opposed to Thr. In a study with model peptides in which Thr was mutated to Ser, no significant changes in substrate production were observed, but a detailed analysis of the different kinetic steps was not performed.[11] The differences observed in our model indicate that k_3 should be larger for Ser, suggesting that this residue is a preferred target for ERK2. However, the final selectivity for Ser or Thr also depends on the different binding affinities for the target peptides and/or dissociation constants of the phosphorylated products. Kinetic studies with target peptides that differ only in the phospho acceptor, Ser or Thr, may help elucidate this aspect of MAPK selectivity.

Role of Lys^{52} in Catalysis. Mutation of a highly conserved Lys in the kinase superfamily has been reported to reduce or totally abolish kinase activity.[46] Lys^{52} of ERK2 interacts with the α- and β-oxygen atoms of ATP (Figure 5A). On the basis of crystallographic evidence, a possible role for the conserved Lys in the positioning of the ATP molecule was suggested.[21] It was shown that mutation of Lys^{52} to Arg distorts the ATP conformation and leads to a kinase with ~5% of the activity of the wild type (WT).[21] However, the Arg side chain overlaps with the ATP binding site and therefore interferes with the binding of the nucleotide,[21] making it difficult to clearly assess the role of Lys^{52}.

We analyzed the role of Lys^{52} in the reaction by generating a neutral Lys^{52}. This model allowed us to asses the relevance of Lys^{52} for catalysis without affecting the conformation of the active site. We conducted constrained optimizations along the previously determined reaction path. Only for the large QM subsystem we were able to obtain stable products, with a large energy difference of 12.9 kcal/mol between the reactants and products, compared with a difference of 3.2 kcal/mol for the WT (Figure 5B). Moreover, the activation barrier of 19.5 kcal/mol was 5.7 kcal/mol higher than in the WT case. The increase in the activation barrier is consistent with experiments in which an ERK2 K52A mutant had less than 0.5% of the activity of the WT protein.[21] Indeed, Robinson et al.[21] showed that Lys^{52} has a small effect on K_m for ATP but an important effect on k_{cat}. In view of these results, it appears that Lys^{52} affects kinase activity primarily by the stabilization of the transition and product states through electrostatic interactions. As we showed before, the Mulliken charge of the ADP moiety becomes more negative as the reaction proceeds. The positive Lys^{52} may thus be important for stabilization of the ADP product during the reaction.

Phosphorylation and Mg^{2+} Cations. Kinases require Mg^{2+} cations as cofactors for efficient catalytic activity. Despite the abundant crystal structures and the kinetic characterization of the reaction mechanism, the actual role that these cations play is still unclear. In our initial model, two Mg^{2+} cations occupying the M1 and M2 positions were considered. In our simulations, the two Mg^{2+} cations retain their positions during the reaction process, and the coordination remains the same except for the binding to the γ-phosphate. The distance between the M1 Mg^{2+} and the binding γ-phosphate oxygen stays the same along the

(46) Kamps, M. P.; Sefton, B. M. *Mol. Cell. Biol.* **1986**, *6*, 751–757.

reaction pathway. In contrast, the distance between the M2 Mg^{2+} and the γ-phosphate oxygen increases from 2.16 to 3.26 Å. According to the calculated Mulliken charges in our models, both Mg^{2+} ions receive charge from the system, $-0.4e$ for the M1 Mg^{2+} and $-0.3e$ for the M2 Mg^{2+}, and these charges do not change significantly during the reaction.

Kinases have been shown to phosphorylate their substrates with only one Mg^{2+} bound.[20] In our initial model, the Mg^{2+} in the M1 site is coordinated by two oxygen atoms from the β- and γ-phosphates of ATP, the acidic oxygen atoms of Asp^{165}, and two water molecules. The Mg^{2+} bound in the M2 site is coordinated by two oxygen atoms from the α- and γ-phosphates of ATP, one oxygen from Asp^{165}, one oxygen from Asn^{152}, and a water molecule. To explore the possibility of catalysis with only one Mg^{2+} ion in the active site, we performed additional calculations. The first question that arises is which of the two binding sites, M1 and M2, is preferentially occupied. Crystallographic studies on PKA, which have been used as the model for analyzing the Ser/Thr kinase family, showed that M1 is the higher-affinity Mg^{2+} site sufficient for catalysis, while the lower-affinity M2 site becomes occupied when the concentration of Mg^{2+} exceeds that for ATP.[42] However, a careful examination of several other Ser/Thr kinase crystal structures showed that a single bound Mg^{2+} can also be found in the M2 site (e.g., in the structures with PDB codes 1HCK, 1J1C, 1JKK, and 1S9I). We noted that the reported Ser/Thr kinases were crystallized with ADP, ATP, or nonhydrolyzable analogues; with or without inhibitors; in active or inactive states; and with or without substrates. This variety precludes a generalization for the whole Ser/Thr kinase family. Moreover, the binding site conformations were significantly different among the different structures. Nevertheless, most of the crystal structures of kinases that have high sequence identity with ERK2 and were crystallized with only one Mg^{2+} had the M2 site occupied instead of the M1 site. Among them, the mutant ERK2 structure 1GOL,[21] where Lys^{52} was mutated to Arg, has one Mg^{2+} bound in the M2 site. In agreement with these observations, when we generated one-Mg^{2+} models with the M1 or M2 Mg^{2+} moved from the catalytic site to the solvent, we found that only when the M2 Mg^{2+} was left in the binding site did the phospho moiety of ATP retain a conformation suitable for catalysis. The model with one Mg^{2+} in the M2 site differed from the two-Mg^{2+} model mainly in the positioning of one oxygen of the β-phosphate that was binding the M1 site; this oxygen rotated and bonded to the M2 Mg^{2+}, in agreement with crystal structures of kinases with only one Mg^{2+} (Figure S1A in the Supporting Information).[47] Interestingly, this result may explain why the k_{cat} toward ELK1 of the ERK2 Asn^{152} to Ala mutant is reduced,[48] as mutation of Asn^{152} may change the binding of Mg^{2+} to the M2 site.

We then used the model with one Mg^{2+} bound at M2 (denoted $1Mg^{2+}$) to analyze the reaction pathway. We followed the same reaction coordinate that we determined for the two-Mg^{2+} model. Interestingly, the reaction mechanism remained similar to that for the two-Mg^{2+} case (Table 1 and Figure S1B in the Supporting Information). The O_1-P_2 distance was slightly increased, which could lead to a weakening of the O_1-P_2 bond. We also analyzed the differences in Mulliken charges along the reaction and found that the M2 Mg^{2+} charge does not change from the two-Mg^{2+} model and is constant during the phospho transfer process. The extra charge previously transferred to the M1 Mg^{2+} was distributed on the ATP, Asp^{147}, and Lys^{149} almost equally. Surprisingly, we found an activation barrier of only 5.0 kcal/mol from the change of potential energy along the reaction coordinate. These effects could be caused by a destabilization of the reactant state, as the second Mg^{2+} strongly interacts with ATP. In summary, our results show that ERK2 is active with one Mg^{2+} bound to the M2 site and that the reaction mechanism seems to be similar to that for the two-Mg^{2+} case. A combination of NMR and QM methods, as used to understand Ca^{2+} binding to calmodulin,[49] may help to clarify these points further.

Conclusions

MAPKs regulate gene expression primarily through the phosphorylation of transcription factors.[50] However, how MAPKs bind and phosphorylate their targets is not yet fully understood. Structural and biophysical aspects of MAPKs have been studied in great detail, with more than 80 structures deposited in the PDB to date.[51] Even though these studies have resulted in a general understanding of the canonical kinase catalytic domain structure, structures of MAPKs with a target bound in the catalytic site have not been determined. A factor probably interfering with crystallization is that the binding sites of MAPKs for their peptide substrates are mostly outside of the catalytic domain.[52] Recent studies have provided compelling evidence that these binding sites for docking motifs play a key role in determining the substrate specificity of MAPKs.[53] Binding to this docking site and the active site usually involves unstructured regions in protein targets, which may be another factor precluding crystallization. Here we constructed a model of the complex between ERK2 and a target peptide based on an extensive set of related kinase structures and tested the model by conducting a QM/MM study of the reaction catalyzed by ERK2. On the basis of the structural model, we propose that the unique characteristics of Pro are the main reasons for MAPK specificity toward Ser/Thr−Pro motifs. In particular, Pro has a medium-sized hydrophobic face, lacks an NH group, and is intrinsically rigid. Its ability to position the target tightly at the right distance also suggests a role for Pro in catalysis. In this regard, the model that we have presented here complements previous structural studies, thus providing further insight into the functional aspects of this key family of protein kinases. Another important characteristic of Ser/Thr−Pro motifs in transcription factors is that they undergo Pro cis−trans isomerization, which can be regulated by the prolylisomerase Pin1 after phosphorylation by MAPKs.[54] The resulting enhancement in transcriptional response to growth factors can be attributed to a modified binding mechanism to their cotranscription factors, indicating that the Ser/Thr−Pro selectivity is used to precisely regulate the MAPK signaling routes.

We used the modeled ERK2−peptide complex to determine the reaction pathway catalyzed by this MAPK. The main

(47) Schulze-Gahmen, U.; De Bondt, H. L.; Kim, S. H. *J. Med. Chem.* **1996**, *39*, 4540–4546.
(48) Zhang, J.; Zhou, B.; Zheng, C. F.; Zhang, Z. Y. *J. Biol. Chem.* **2003**, *278*, 29901–29912.
(49) Biekofsky, R. R.; Turjanski, A. G.; Estrin, D. A.; Feeney, J.; Pastore, A. *Biochemistry* **2004**, *43*, 6554–6564.
(50) Turjanski, A. G.; Vaque, J. P.; Gutkind, J. S. *Oncogene* **2007**, *26*, 3240–3253.
(51) Lee, S. J.; Zhou, T.; Goldsmith, E. J. *Methods* **2006**, *40*, 224–233.
(52) Lee, T.; Hoofnagle, A. N.; Kabuyama, Y.; Stroud, J.; Min, X.; Goldsmith, E. J.; Chen, L.; Resing, K. A.; Ahn, N. G. *Mol. Cell* **2004**, *14*, 43–55.
(53) Dimitri, C. A.; Dowdle, W.; MacKeigan, J. P.; Blenis, J.; Murphy, L. O. *Curr. Biol.* **2005**, *15*, 1319–1324.
(54) Monje, P.; Hernandez-Losa, J.; Lyons, R. J.; Castellone, M. D.; Gutkind, J. S. *J. Biol. Chem.* **2005**, *280*, 35081–35084.

findings are that the reaction occurs in one step, with the Ser/Thr H^+ being transferred to a conserved Asp at the end of the reaction. On the basis of previous QM/MM calculations on PKA[16,44] and CDK2,[45] two different mechanisms have been proposed. In the PKA calculations,[16,44] the proton from the alcoholic amino acid was found to be transferred to a conserved Asp, while for CDK2,[45] it was transferred to a phosphate of the ATP. Our results align with the previous studies on PKA[16,44] and contrast to the results on CDK2.[45] An activation barrier of 10 kcal/mol and a symmetrical transition state was found in the original work of Cheng et al.[16] by performing constraint optimizations along a proposed reaction pathway. Later, Valiev et al.[44] conducted a study on PKA using a QM/MM implementation of the nudged elastic band (NEB) method where no implicit assumption of the reaction coordinates was used. In this case, an activation barrier of 15 kcal/mol and an overall similar transition state were determined. In agreement with the two studies on PKA, we find that the proton transfer occurs late in the reaction pathway. As stated above, the main differences arise with a Car−Parrinello QM/MM study[45] that proposed an associative phosphoryl transfer with a 24 kcal/mol activation barrier. The position of two key residues that are conserved in the kinase superfamily, Asp^{147} and Lys^{149} in ERK2, could account for the observed differences. In the crystal structures of PKA with ADP, aluminum fluoride, and a substrate peptide (1L3R[55]) and CDK2 with ATP and a substrate peptide (1QMZ[33]), the target serine is located between the Asp and Lys residues, thus precluding the formation of a salt bridge between them. However, in the CDK2 study,[45] a salt bridge formed upon molecular dynamics relaxation of the complex. The interaction with Lys likely reduces the proton affinity of Asp, thus eliminating it as the catalytic base. In contrast, here and in the PKA studies,[16,44] the salt bridge is not formed, and the Asp is free to accept the proton from the Ser/Thr residue. Interestingly, in a structure of PKA similar to 1L3R[55] but with a bound inhibitor that lacks the Ser residue (1ATP[42]), the distance between the conserved Asp and Lys residues is 3.4 Å, almost 1 Å shorter than in the 1L3R structure.[55] On the basis of these results from simulations and experiment, we propose that the presence or absence of the salt bridge between Asp and Lys likely determines the proton acceptor and thus an important aspect of the kinase reaction mechanism.

The QM/MM methodology allowed us to explore the energetic feasibility of proposed reaction mechanisms and to analyze the role of different groups within the active site. We determined that a similar mechanism is employed for both Ser and Thr but that Ser phosphorylation has a lower activation barrier than that for Thr. This difference may be a regulating factor in targets with similar binding affinities. Our study also sheds light on the role of Lys^{52}, a conserved residue in subdomain II whose mutation is often used to confirm kinase activity of novel gene products. We propose that this conserved Lys stabilizes the ADP moiety being formed in the transition and product states in addition to positioning the ATP in a conformation conducive to the phosphoryl transfer. We showed that ERK2 is able to phosphorylate its targets even in the presence of only one Mg^{2+} in the M2 position, in agreement with previous experiments,[20] and that the reaction mechanism remains essentially unchanged, which helps explain why many kinases are active in the presence of low magnesium concentrations.

QM/MM methods are typically used in structures that have detailed information about the active site. In this study, we were able to reconstruct the whole active site on the basis of the wealth of structural information available for the kinase superfamily. Good correlation with experiments suggests that this is a reasonable approach. Modeling techniques aimed at understanding protein reaction mechanisms in detail can be extended to cases where the structure of the complex has not been resolved if enough structural and biochemical data are available.

In summary, we constructed a model of the complex of ERK2, ATP, and a target peptide bound to the active site and used it to analyze in detail the reaction catalyzed by the MAPK ERK2. As kinases from different families share a similar catalytic site, a consensus mechanism could be expected; however, differences may arise as a result of slight conformational changes, specific restraints, or substitution of the intervening groups not necessarily directly involved in catalysis. Thus, similar studies on other kinase families may shed additional light on the mechanisms whereby kinases transfer the phospho group from ATP to their specific protein targets.

Acknowledgment. Adrian Turjanski was supported as a PEW Latin American Fellow. The authors acknowledge support by the Intramural Research Programs of NIDCR, NIH (A.G.T. and J.S.G.) and NIDDK, NIH (G.H.).

Supporting Information Available: Structure of the $1Mg^{2+}$ complex, a plot of the changes in the most relevant distances during the reaction of $1Mg^{2+}$, the coordinates (in PDB format) of the ERK2 complex used for the QM/MM calculations, and complete refs 22 and 26. This material is available free of charge via the Internet at http://pubs.acs.org.

JA8071995

(55) Madhusudan; Akamine, P.; Xuong, N.-H.; Taylor, S. S. *Nat. Struct. Biol.* **2002**, *9*, 273–277.